Nonlinear Iris Deformation Correction Based on Gaussian Model

Zhuoshi Wei, Tieniu Tan, and Zhenan Sun

Center for Biometrics and Security Research
National Laboratory of Pattern Recognition, Institute of Automation
Chinese Academy of Sciences. P.O. Box 2728, Beijing, P.R. China, 100080
{zswei,tnt,znsun}@nlpr.ia.ac.cn

Abstract. Current iris recognition systems can achieve high level of success under restricted conditions, while they still face challenges of utilizing images with heavy deformation caused by illumination variations. Developing methods to alleviate the deformation becomes a necessity, since the requirement of uniform lighting is often not practical. This paper introduces a novel algorithm to counteract elastic iris deformation. In the proposed algorithm, for nonlinear iris stretch, the distance of any point in the iris region to the pupil boundary is assumed to be the corresponding distance under linear stretch plus an additive deviation. Gaussian function is employed to model the deviation. Experimental results on two databases with nonlinear deformation demonstrate the effectiveness of the algorithm. The proposed iris deformation correction algorithm achieves a lower Equal Error Rate (EER), compared to the other two linear and nonlinear normalization methods in the literature, making the system more robust in realistic environments.

1   Introduction

Since last decade, researchers have put great efforts in automatical personal identification based on biometrics. Iris pattern is considered as one of the most reliable biometric modalities due to the abundant distinctive information preserved in the iris texture. Current iris recognition systems can achieve good performance under restricted conditions. However, they still encounter challenges in realistic environments with significantly large illumination variations. Pupil dilation and contraction caused by illumination change make the iris texture undergoes nonlinear deformation. Iris normalization is important to iris recognition as it intends to reduce the effect of iris deformation. As the majority of iris recognition systems employ linear normalization, which is unsatisfactory in handling nonlinear iris distortion, it is necessary to develop nonlinear normalization methods to counteract the deformation.

Although iris recognition has been investigated over the past decade, only a few works focus on the deformation issue. Daugman [1] used a Rubber-sheet model based normalization which linearly project the annular iris region into a fixed rectangle: $I(x(r, \theta), y(r, \theta)) \rightarrow I(r, \theta)$. Yuan and Shi [2] employed a iris
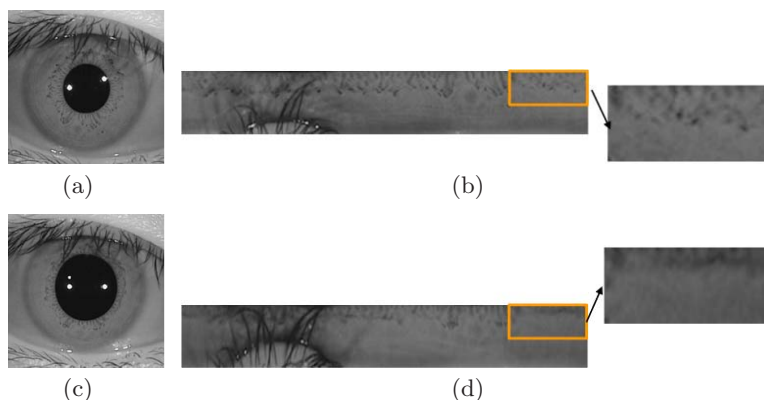
Fig. 1. Deformed image samples which can not align well under linear normalization

meshwork model proposed by Wyatt [3], and from which they deduced the relationship of iris collagen fibers between different pupil sizes. Li [4] used local calibration to alleviate iris distortion. Most of the existing systems employ Daugman's [1] linear iris normalization algorithm. However, some heavily deformed images still pose a challenge to linear normalization. Fig. 1 shows an example. Fig. 1(a) and Fig. 1(c) are two images captured from the same iris, but with very different pupil sizes. They can not align well under linear normalization, which is shown in Fig. 1(b) and Fig.1(d), especially in the zoomed region.

Human iris is an internal organ that is visible externally. The movement of iris (mainly dilation/contraction) controls the pupil size and thus dominates the amount of light that enter the eye through the pupil. According to [3], pupil diameter may range from a minimum of about 1.5mm to a maximum of over 7mm. Such distortion of iris texture may enlarge intra-class variations or increase the False Reject Rate (FRR). A major goal of this paper is to introduce a novel method to compensate elastic iris deformation. Motivated by Wyatt's [3] iris mesh model, we use a nonlinear deformation correction algorithm that utilizes Gaussian function to approximate the additive deviation of nonlinear iris stretch. The effectiveness of the algorithm is confirmed by experiments on two databases, both of which are collected under illumination changes. Our method achieves better recognition performance than the other two methods.

The rest of this paper is organized as follows. Section 2 describes the proposed nonlinear deformation correction algorithm. Section 3 gives the experimental results and discussion. Section 4 concludes the paper.

2 Nonlinear Iris Deformation Correction

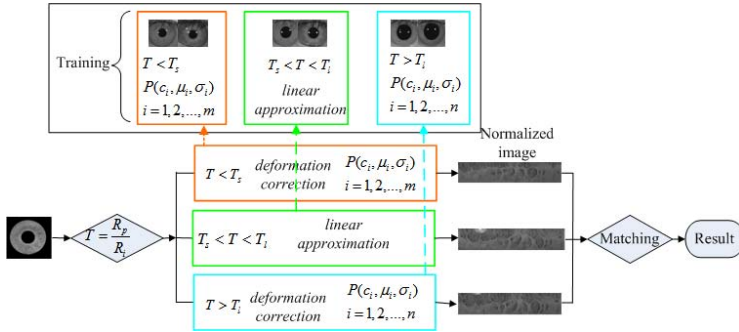A complete framework of iris recognition system with deformation correction is plotted in Fig. 2.

Fig. 2. The framework of iris recognition system with deformation correction

2.1   Iris Model

Iris collagen fibers are generally considered as radial components, which is also the assumption made by linear normalization methods. With the stretch of these radial fibers, the fibers near pupil boundary would undergo larger deformation than those fibers near iris boundary. One disadvantage of this assumption lies in the contradiction that iris structure requires very good mobility whereas iris collagen fibers are relatively inextensible tissues.

In this paper, we employ a meshwork "skeleton" of iris structure which was proposed by Rohen [5]. In the "skeleton" model, a series of fibrous arcs (left arcs and right arcs) which connect pupil boundary and iris boundary are inter-weaving together to form iris structure, as Fig. 3 shows. We do not consider iris meshwork model as exactly the human iris structure. But we believe that it is more reasonable in two aspects: first, this structure is much more complicated than the over-simplified radial one. It is highly flexible and fits for the pupil movements. Second, while the radial fibers go through acute change with pupil diameter varies, which makes people easy to feel fatigable, the meshwork model provides a possibility that the length of each arc undergoes less change.

As the meshwork model is also employed by Yuan and Shi [2], we give a brief comparison to these two employments. In Yuan's method, they made several assumptions: 1, the angles (θ in Fig. 4(a)) that correspond to iris fibrous arcs is 90°; 2, the fibrous arcs are part of circle so that the relationship between linear and nonlinear stretch can be acquired by solving two equations of circles. In the proposed method, we do not make such constraints because the angle θ would hardly remain constant and fibrous arcs would hardly remain as circles during the frequent change of pupil diameter. Instead we use a flexible assumption (Eq. 1) and acquire iris deformation model by statistical learning. Experimental results show that the proposed method is more reasonable in dealing with the deformation problem.

Fig. 4(a) illustrates the basic idea of the meshwork model. Suppose the solid line in Fig. 4(a) represents one fibrous arc in linear stretch model, and the dashed line represents the same arc in nonlinear stretch model. In Wyatt's treatment
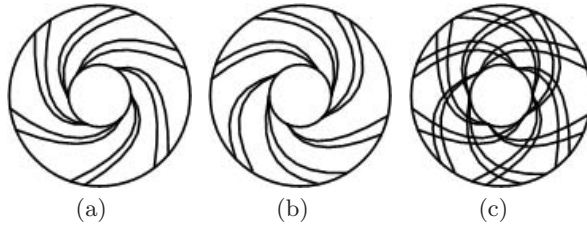
Fig. 3. Iris meshwork model described by Rohen [5]. (a) Left arcs. (b) Right arcs. (c) The meshwork model.
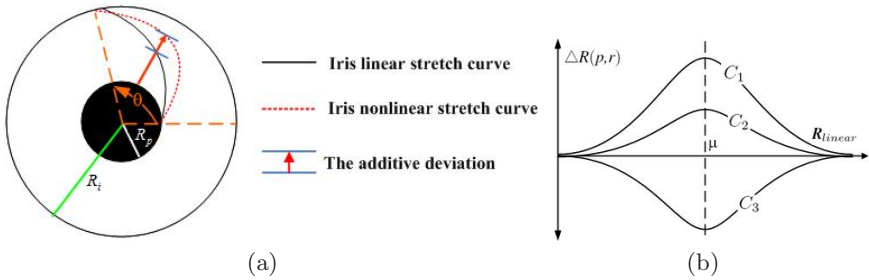

Fig. 4. (a) The relationship between linear and nonlinear iris stretch in Wyatt's work [3]. (b) The Gaussian model for additive deviation.

[3] to nonlinear stretch, a point in any position of iris region can be described as:

$$R_{nonlinear} = R_{linear} + \triangle R(p,r), \tag{1}$$

where R_{linear} is the position in linear stretch, and $\triangle R$ is the additive deviation related to R_{linear} (denotes as r) and pupil dilation (denotes as p). This deviation is described by a 6th-order polynomial in Wyatt's work [3], which is somewhat arbitrary as long as it is smooth enough to provide any flexibility to support elastic iris deformation.

2.2 Additive Deviation in Nonlinear Iris Stretch

As mentioned by Wyatt [3], the treatment described by Eq.1 is proved to be the easiest using fractional radial position instead of absolute radial position as a variable. Fractional position is defined as:

$$f = \frac{R - R_p}{R_i - R_p}, \tag{2}$$

here R is the distance of any point in iris region to the pupil center. R_p and R_i denote pupil radius and iris radius respectively, as Fig. 4(a) shows. In the remaining part of this paper, we use fractional position to refer to each variable in Eq.1.

In linear stretch, the fractional position of a fixed point is invariant as pupil size varies, therefore linear fractional position R_{linear} is an easily determined part. The key problem is how to model the additive deviation $\triangle R$. As the 6th-order polynomial is computationally expensive in real-time applications, we intend to find a simple way to express $\triangle R$ that can make the system both efficient and accurate.

Generally speaking, $\triangle R$ can be model as a function of pupil radius R_p and linear fractional position R_{linear}, since iris radius R_i is a relatively stable variable. However, due to the flexible distance from the camera during image acquisition, iris radius R_i often presents different values. Considering the influence of R_i, we use the ratio of pupil radius to iris radius $T = \frac{R_p}{R_i}$ to measure the degree of iris deformation. Therefore, in the proposed algorithm, we assume that $\triangle R$ is a function of R_{linear} and T, denoted as $\triangle R(R_{linear}, T)$.

2.3   Choice of Iris Deformation Factor

Pupil diameter undergoes small oscillations ("hippus") once or twice per second, even under uniform lighting. Weak illumination causes pupil dilation and increases the ratio T whereas intense illumination causes pupil contraction and decreases T. Iris takes much more deformation in dark and bright environment than in normal environment. According to our statistics, the ratio T of most irises stay in an interval $[T_s, T_l]$ under uniform lighting. In the proposed method, we use linear normalization to approximate iris stretch when T is in the threshold $[T_s, T_l]$. Otherwise, iris images are treated as nonlinear stretch.

As a measuring parameter, when $T > T_l$, pupil dilates and iris compresses. The larger T is, the heavier iris deforms. On the contrary, when $T < T_s$, pupil contracts and iris extends. The smaller T is, the heavier iris deforms. In the proposed algorithm, we set $(\frac{T_s + T_l}{2} - T)$ as a factor of the additive deviation $\triangle R$, indicating how heavily the deformation is while compared to the non-deformed images. However, the choice of this deformation factor is not unique. Here we assume the deviation is described as:

$$\triangle R = C \times F(R_{linear}), \tag{3}$$

here $C = (\frac{T_s + T_l}{2} - T)$, and $F(R_{linear})$ is a function of R_{linear}.

2.4   The Gaussian Model for Deviation

As how to model iris collagen fibers movement is still an open problem, we learn $F(R_{linear})$ via training. The training data set: $D_{k,m} = \{D_{i,j} | i = 1, 2, ..., k; j = 1, 2, ..., m\}$ contains 600 iris images with $k = 10$ subjects, and each subject has an image sequence which contains $m = 60$ images captured under gradually varying illumination. Some image samples are shown in Fig. 6(a). We apply the following procedure to obtain $F(R_{linear})$:

1. Given an image sequence: $D_i = \{D_{i,1}, D_{i,2}, ..., D_{i,m}\}$, we mark n prominent points on every iris image (shown in Fig. 6(a)) and obtain their nonlinear stretch positions $R_{nonlinear}$ by measuring the distance between each point and the pupil boundary.
2. Divide iris region into three annular regions equally, as illustrated in Fig. 6(b). According to their distance to pupil boundary, we use three sets $\{P_{in}\}$, $\{P_{mid}\}$ and $\{P_{out}\}$, respectively, to denote the location within each region.
3. Group all the points into the three sets $\{P_{in}\}$, $\{P_{mid}\}$ or $\{P_{out}\}$ using the Nearest Neighbor clustering method.
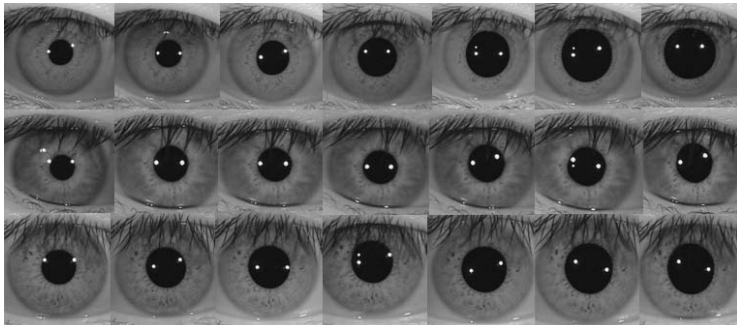

Fig. 5. Iris image samples with heavy elastic deformation

As nonlinear stretch positions $R_{nonlinear}$ is obtained by locating the points manually and linear stretch positions R_{linear} is approximated by iris stretch under uniform lighting, $\triangle R$ can be acquired by simply applying Eq. 1. Fig. 6(c) depicts the relationship between $\triangle R$ and pupil dilation $T = \frac{R_p}{R_i}$. It shows that when pupil size is appropriate (T is around 0.47), the deviation reaches the lowest. When pupil contracts, $\triangle R$ presents a positive deviation. Otherwise pupil dilates and $\triangle R$ presents a negative deviation.

Fig. 6(c) also shows that the degree of deformation is varying from regions. Texture in the middle region $\{P_{mid}\}$ suffers more deformation than texture near pupil/iris boundary (regions $\{P_{in}\}/\{P_{out}\}$). We rearrange the value of $\triangle R$ to estimate its relation to R_{linear}, shown in Fig. 6(d), which expresses iris deformation from another perspective.

The relationship between $\triangle R$ and R_{linear} can be approximated as Gaussian function (solid line in Fig. 6(d)), with the mean around the center of R_{linear}. $\triangle R$ apparently should be equal to 0 at pupil boundary or iris boundary, that is to say, the additive deviation should be subjected to: $\triangle R = 0$, when $R_{linear} = 0$ or 1. In this case σ should be chosen less than $\mu/3$, so that $N(\mu, \sigma^2)$ is out of the interval of $[\mu - 3\sigma, \mu + 3\sigma]$, which leads to $\triangle R \approx 0$ when $R_{linear} = 0$ or 1. In the proposed algorithm, μ and σ are learned from training while obeying these rules.

The index C_i $(i = 1, 2, 3, \cdots)$ in Fig. 6(d) is the deformation factor described in Eq. 3, indicating the degree of deformation. For each different C, there is a

different curve to represent the deviation. If $C > 0$, pupil contracts, iris extends, and $\triangle R$ appears to be a positive deviation. On the contrary, $C < 0$, pupil dilates, iris compresses, and $\triangle R$ appears to be a negative deviation.

Finally $F(R_{linear})$ is expressed as Gaussian function, and a deformed image can be corrected by compensating the additive deviation $\triangle R$, which can be described as:

$$\triangle R = C \times F(R_{linear}) = C \times N(\mu, \sigma^2)$$
$$= C \times \frac{1}{\sqrt{2\pi}\sigma} \exp\{-\frac{(R_{linear} - \mu)^2}{2\sigma^2}\}. \tag{4}$$

Once the additive deviation $\triangle R$ is chosen as Gaussian function, shown in Fig. 4(b), nonlinear iris stretch model is able to be measured. The fractional position of each point under nonlinear stretch is computed based on Eq. 1. According to Eq. 4, every deformed image has 3 parameters to be determined. We denote these parameters as $P(c_i, \mu_i, \sigma_i)$, which is mentioned in our framework (see Fig. 2).
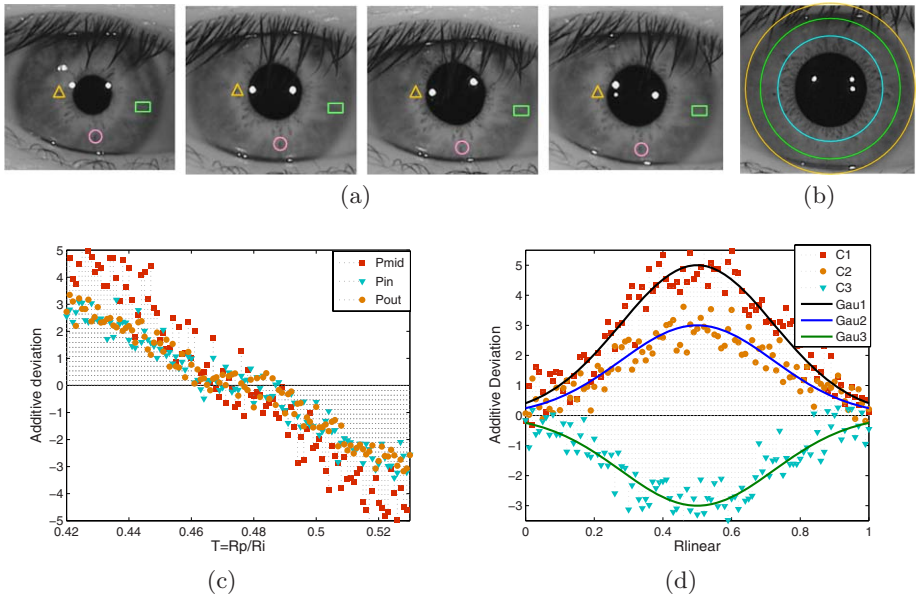

(a)   (b)

(c)   (d)

Fig. 6. Illustration of training. (a)Recording the location of iris prominent points. (b)The three annular regions. (c)The relationship between $\triangle R$ and $T = \frac{R_p}{R_i}$. (d)The relationship between $\triangle R$ and R_{linear}.

3   Experiments and Discussion

In this section the proposed nonlinear iris deformation correction algorithm is evaluated on two databases, both of which possess large pupil size variations.

We incorporated the proposed algorithm with Daugman's [1] iris localization and Ma's [6] feature extraction algorithm into one recognition system. To eliminate other influences, we only adopt clear images in the experiment. Daugman's Rubber-sheet model and Yuan's nonlinear normalization are also implemented on the same database for comparison.

3.1   Experiments on DB1

To evaluate the effectiveness of the proposed algorithms in different lighting condition, we collected a database (denote as DB1) under gradually changing illumination using a hand held device produced by OKI. It contains 30 classes and each class contains 60 images. Samples of 3 subjects' images are given in Fig.5, which shows that there is heavy deformation within each class. $T = \frac{R_p}{R_i}$ ranges from a minimum of 0.2353 to a maximum of 0.5902 in DB1. The within class deformation in DB1 is heavier than any other publicly available databases, therefore it is quite challenge. Ten arbitrary classes are selected for training, leaving
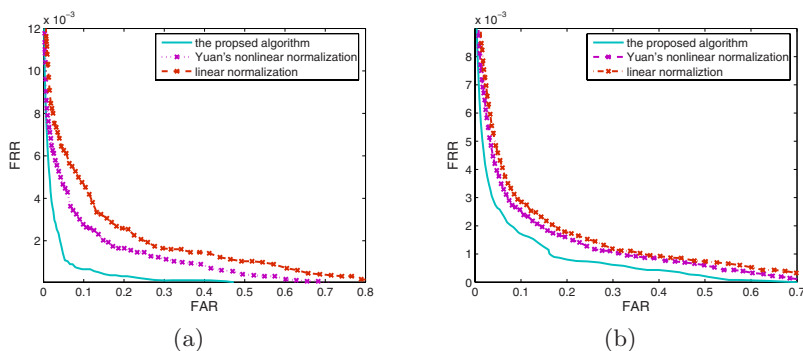

Fig. 7. (a) ROC curve in DB1. (b) ROC curve in CASIA-IrisV3-Lamp
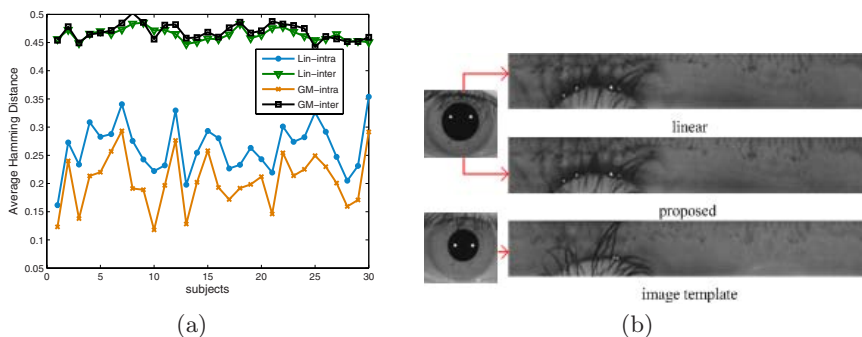

Fig. 8. (a) Hamming distance (HD) of Linear(Lin) method vs. Gaussian model(GM) correction. (b) A sample iris texture with GM correction that align better with the image template. (Lin vs. Tem: 0.459HD; GM vs. Tem: 0.375HD)

the rest 20 classes for testing. All possible intra-class and inter-class comparisons are made to evaluate the recognition performance. The ROCs (receiver of operating curves) of the three methods are shown in Fig.7(a). The EER (equal error rate) and discriminating index [1] ($DI = \frac{|\mu_1 - \mu_2|}{\sqrt{\frac{(\sigma_1^2 + \sigma_2^2)}{2}}}$) are shown in Table 1. The benefits of our approach are well illustrated in Fig. 8(a), which plots the average intra/inter-class Hamming distances of the 30 classes in DB1. This figure shows that our method can reduce the intra-class distance while maintaining the inter-class distance. Fig. 8(b) shows a corrected iris sample that align better with the image template in the case of a genuine match.

3.2 Experiments on CASIA-IrisV3-Lamp Database

To get a more convincing result, our second experiment is based on a larger database. We take 400 classes of iris images from CASIA-IrisV3-Lamp [7] database. Each class contains 20 images, 10 of which were captured with a lamp on and the other 10 with the lamp off. So images of this database also contain nonlinear deformation due to the variation of visible illumination. By excluding the poor quality image data, only three quarters of the total images are employed in the experiment. The ROCs are shown in Fig. 7(b). The EER and DI are shown in Table 2.

3.3 Discussion

The experimental results demonstrate that the proposed deformation correction algorithm using Gaussian model outperforms the other two methods, by obtaining a lower EER and higher discriminating index. While Daugman's [1] Rubber-sheet model linearly projects iris region into a rectangle, the proposed Gaussian deformation correction model makes use of iris structure and it can better alleviate the distortion. Compare to Yuan's [2] nonlinear normalization, the proposed method uses a more simple and flexible approach, but achieves better results, therefore it is more effective in correcting iris deformation.

Table 1. EER and DI on DB1

	Daugman	Yuan	Proposed
EER	1.058%	0.857%	0.733%
DI	4.7094	4.8213	4.9913

Table 2. EER and DI on CASIA-IrisV3-Lamp

	Daugman	Yuan	Proposed
EER	0.973%	0.831%	0.719%
DI	4.7509	4.8409	4.9083

4   Conclusion and Future Work

In this paper, we have proposed a novel method to correct nonlinear iris deformation. In this algorithm, iris images are corrected by compensating the additive

deviation between nonlinear and linear iris stretch. The additive deviation is described by Gaussian function, which is chosen via training. Experimental results demonstrate that the proposed algorithm can resist considerable iris deformation and yield better results than the other two approaches. Therefore it makes iris recognition system more robust to the external stimulus, such as illumination variations.

How to deal with iris deformation problem has only been addressed by a few literatures, and we think this issue hold great importance in iris recognition. In the future, we will try to tackle the problem not only from iris model but also the appearance of iris images. Hopefully it can deepen our understanding of iris deformation and improves the recognition performance.

Acknowledgement

References

1. Daugman, J.: High confidence visual recognition of persons by a test of statistical independence. IEEE Transactions on Pattern Analysis and Machine Intelligence 15(11), 1148–1161 (1993)
2. Yuan, X., Shi, P.: A non-linear normalization model for iris recognition. In: Advances in Biometric Person Authentication, pp. 135–141 (2005)
3. Wyatt, H.J.: A 'minimum-wear-and-tear' meshwork for the iris. Vision Research 40, 2167–2176 (2000)
4. Li, X.: Modeling intra-class variation for nonideal iris recognition. In: International Conference on Biometrics 2006, pp. 419–427 (2006)
5. Rohen: Der bau der regenbogenhaut beim menschen undeinigen saugern. Gegenbaur Morphology Journal 91, 140–181 (1951)
6. Ma, L., Tan, T., Wang, Y., Zhang, D.: Personal identification based on iris texture analysis. IEEE Transactions on Pattern Analysis and Machine Intelligence 25(12), 1519–1533 (2003)
7. CASIA-IrisV3: `http://www.cbsr.ia.ac.cn/IrisDatabase.htm`